

# Measuring the speed of light using beating longitudinal modes in an open-cavity HeNe laser

Daniel J. D’Orazio,<sup>\*</sup> Mark Pearson, Justin T. Schultz,<sup>†</sup> Daniel Sidor,<sup>‡</sup> Michael Best,<sup>§</sup> Kenneth Goodfellow, Robert E. Scholten,<sup>¶</sup> and James D. White<sup>\*\*</sup>  
*Juniata College, Department of Physics, Huntingdon, Pennsylvania 16652*

We describe an undergraduate laboratory that combines an accurate measurement of the speed of light, a fundamental investigation of a basic laser system, and a nontrivial use of statistical analysis. Students grapple with the existence of longitudinal modes in a laser cavity as they change the cavity length of an adjustable-cavity HeNe laser and tune the cavity to produce lasing in the TEM<sub>00</sub> mode. For appropriate laser cavity lengths, the laser gain curve of a HeNe laser allows simultaneous operation of multiple longitudinal modes. The difference frequency between the modes is measured using a self-heterodyne detection with a diode photodetector and a radio frequency spectrum analyzer. Asymmetric effects due to frequency pushing and frequency pulling, as well as transverse modes, are minimized by simultaneously monitoring and adjusting the mode structure as viewed with a Fabry-Perot interferometer. The frequency spacing of longitudinal modes is proportional to the inverse of the cavity length with a proportionality constant equal to half the speed of light. By changing the length of the cavity, without changing the path length within the HeNe gas, the speed of light in air can be measured to be  $(2.9972 \pm 0.0002) \times 10^8$  m/s, which is to high enough precision to distinguish between the speed of light in air and that in a vacuum.

## I. INTRODUCTION

Lasers emit light over a range of wavelengths described by the laser line shape function.[1–3] For a HeNe laser operating under normal conditions, the main source of laser line shape broadening is Doppler broadening in the lasing medium, resulting in a Gaussian gain profile (see Fig. 1). The laser does not emit a continuous spectrum of wavelengths over this Gaussian gain-permitted wavelength range; rather, it can only lase when there is resonance in the lasing cavity. For the TEM<sub>00</sub> mode there exists an integer number,  $N$ , of half wavelengths between the mirrors of the laser cavity, resulting in the allowed resonance wavelengths

$$\lambda_N = \frac{2nL}{N}, \quad (1)$$

where  $L$  is the length of the laser cavity and  $n$  is the index of refraction of the medium filling the laser cavity.

The laser output consists of discrete wavelength peaks with power dictated by the Gaussian line shape envelope and the unsaturated gain threshold (see Fig. 1). These peaks are called longitudinal cavity modes. When the

laser cavity supports more than one peak (that is, where the gain is greater than the losses for those peaks), the laser output consists of multiple discrete wavelengths. If the light from these multiple modes is projected onto a detector (for example, a photodiode), then the photocurrent will oscillate at the difference frequency, producing a beat signal.

The beat frequency of interest is at the frequency due to the spacing between adjacent longitudinal modes. The frequency of the  $N$ th mode can be derived from Eq. (1) to be  $f_N = N(c/2nL)$ . Thus the beat frequency is given by

$$\Delta f = \frac{c}{\lambda_{N+1}} - \frac{c}{\lambda_N} = \frac{c}{2nL}, \quad (2)$$

and therefore  $L = c/2n\Delta f$ , indicating that the cavity length is directly proportional to the reciprocal of the beat frequency.[4] Observing the variation in beat frequency between adjacent longitudinal modes with the cavity length  $L$  gives the speed of light.

Accurate measurements of the beat frequency are accomplished inexpensively by directing the output of the laser onto a high-speed photodetector[5] monitored with an RF spectrum analyzer or frequency counter.[6–8] This approach has been demonstrated in Ref. 9 in an undergraduate experiment with the goal of measuring the speed of light using the relation in Eq. (2) for a single laser cavity length and single corresponding beat frequency. The method is easily understood because it is analogous to investigations of waves on a string. It has a drawback, however; the inability to obtain a precise measurement of the cavity length (from the inner-cavity side of the output coupler to inner-cavity side of the back mirror) inevitably leads to results that are only marginally better than those obtained with standard time-of-flight or Foucault methods commonly used in undergraduate physics laboratories, which typically yield measurements

<sup>\*</sup>A 2009 graduate of Juniata College currently supported by a Fulbright Fellowship at the University of Zürich.

<sup>†</sup>A 2008 graduate of Juniata College and 2008–2009 Fulbright Fellow at the Australian National University. He is now doing graduate work at the Optics Institute, University of Rochester.

<sup>‡</sup>A 2007 graduate of Juniata College currently doing graduate work at the Optics Institute, University of Rochester.

<sup>§</sup>A 2006 graduate of Juniata College currently doing graduate work at the University of Pittsburgh School of Medicine.

<sup>¶</sup>ARC Centre of Excellence for Coherent X-ray Science, School of Physics, The University of Melbourne, Victoria 3010, Australia.

<sup>\*\*</sup>Electronic address: white@juniata.edu

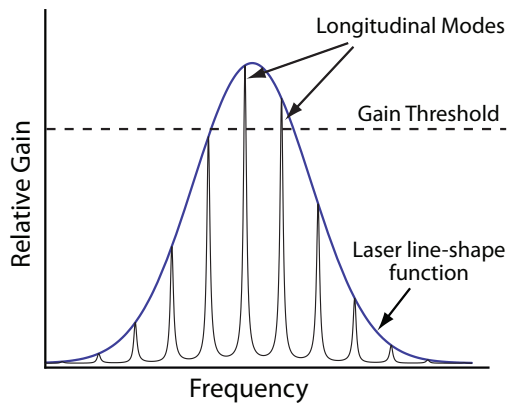


FIG. 1: Schematic illustration of the longitudinal cavity modes and gain bandwidth of a laser. In the situation shown, the net gain minus losses is sufficient for laser output at only two longitudinal cavity modes. The beat frequency that we observe to measure the speed of light is the spacing between these adjacent modes.

accurate to within  $\approx \pm 1\%$ . [10–12] Minor improvements on this method can be made by collecting data for multiple lasers of different lengths and plotting the beat frequency as a function of cavity length. In addition to the uncertainty in length between the mirrors, there is also the problem of not knowing a precise (and constant) value for the index of refraction inside the gas tube. These obstacles can be overcome by using the laser as a simple light source, amplitude modulated at the inter-mode beat frequency, and measuring the phase difference between detectors placed at two different locations along the laser path. [13] This modulation technique improves the measurement of the speed of light by an order of magnitude, but at the cost of increasing the conceptual complexity. The introduction of the adjustable-length HeNe laser significantly reduces the consequences of uncertainty in mirror location and the index of refraction, and improves the measurement by an order of magnitude over the modulation technique, while retaining the conceptual simplicity of the original study of Ref. 9.

## II. METHODS

Figure 2 represents a schematic of the experimental set-up. The laser has an adjustable, open-cavity design with a 28 cm HeNe plasma tube terminated on one side with a mirror and on the other with a Brewster window. The Brewster window suppresses modes with polarization orthogonal to the Brewster plane, so that all supported modes have the same polarization and thus mix effectively in the photodetector. [1, 2] The experiment can be conducted without a Brewster window, but due to mode competition, adjacent longitudinal modes are typically polarized orthogonal to each other and do not mix in the photodetector, resulting in an observed signal with twice the expected frequency. [14] If a Brewster window

is not present, the situation can be remedied by placing a linear polarizer in front of the photodetector to project the polarizations of adjacent modes onto a common axis.

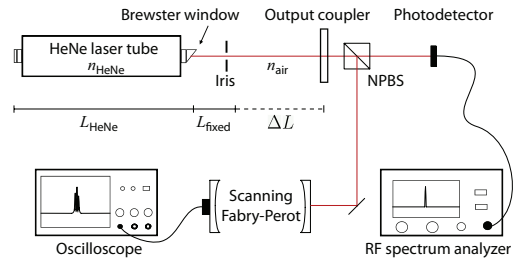


FIG. 2: A schematic of the experimental set-up. The length of the cavity can be adjusted over a range of approximately 16 cm by sliding the output coupler along an optical track. The mode structure of the laser output is monitored using a scanning Fabry-Perot interferometer with a free spectral range of 1.5 GHz and a Finesse of 250. The mode structure is controlled via an adjustable iris in the cavity. The portion of the beam that is not analyzed by the Fabry-Perot is incident on a fast photodetector (1 ns rise time), which is coupled to an RF spectrum analyzer on which the beat signal between adjacent longitudinal modes is observed. (NPBS = non-polarizing beam splitter.)

The variable-length cavity system has been reported and widely used in undergraduate labs to explore laser cavity modes and stability. [15–18] The output coupler is a 0.60 m radius-of-curvature mirror held in a gimbal mount. It is attached to a sliding track, allowing the cavity length to be changed from  $\approx 38$  cm (lower bound limited by the length of the plasma tube) up to  $\approx 54$  cm (upper bound restricted by laser losses). Typically we see two or three longitudinal modes separated by about 300 MHz within the 1.5 GHz gain bandwidth of the HeNe medium. [3] Inside the cavity, between the output coupler and the plasma tube, is an iris used to restrict gain in the region away from the optical axis of the cavity and thus force the laser to emit in the  $TEM_{00}$  (Gaussian) mode. Restricting the laser to a single transverse mode is necessary because higher-order modes produce additional beat frequencies that complicate the RF spectrum. The allowed frequencies for the  $TEM_{00}$  mode are given by Eq. (1), and the allowed frequencies for higher-order  $TEM_{ij}$  modes are given by

$$f_{Nij} = \frac{c}{2L} \left[ N + \frac{1}{\pi} (i + j + 1) \cos^{-1}(\sqrt{g_1 g_2}) \right], \quad (3)$$

where  $N$  is the same mode number as in Eq. (1) and  $g_1 g_2$  is the resonator stability. [2, 19] Thus if  $TEM_{00}$  and  $TEM_{ij}$  are allowed to exist simultaneously in the cavity, beat frequencies will exist at  $c/2L$  and  $c/2L \pm (1/\pi)(i + j + 1) \cos^{-1} \sqrt{g_1 g_2}$ . These additional beat frequencies could provide an interesting method for measuring the resonator stability,  $g_1 g_2$ , for a fixed cavity length.

### A. Cavity Length Measurement

As noted in Sec. I, we cannot accurately measure the entire laser cavity length due to the uncertainty of the position of the mirror in the HeNe tube. In addition, the index of refraction within the He- and Ne-filled tube is different from that in the rest of the cavity, which is filled with air (and a small length of glass at the window). Because we do not know the index of refraction inside the laser plasma tube, we modify Eq. (2) by splitting  $L$  into the two main regions within the laser cavity that have different indices of refraction. Let  $n_{\text{HeNe}}$  be the index of refraction inside the laser plasma tube and  $n_{\text{air}}$  be the index of refraction of air between the Brewster window and the output coupler. Then,  $nL = n_{\text{HeNe}}L_{\text{HeNe}} + n_{\text{air}}L_{\text{air}}$ , where additional fixed components such as the glass window and dielectric mirror coatings are assumed in the first term. In practice neither of these  $L$  values is simple to measure accurately, and thus we split  $L_{\text{air}}$  further into two arbitrary pieces (a fixed length and a measured variable length) such that  $nL = n_{\text{HeNe}}L_{\text{HeNe}} + n_{\text{air}}[L_{\text{fixed}} + \Delta L]$  (see Fig. 2). We substitute this expression into Eq. (2) and obtain

$$\Delta L = \frac{c}{2n_{\text{air}}\Delta f} - \frac{n_{\text{HeNe}}}{n_{\text{air}}}L_{\text{HeNe}} - L_{\text{fixed}}, \quad (4)$$

which is the equation of a line with slope  $c/2n_{\text{air}}$ . Equation (4) allows us to measure the cavity length to an arbitrarily chosen reference point fixed between the laser plasma tube output and the output coupler. In practice we measure  $\Delta L$  from a fixed block near the sliding track to the base of the output coupler using digital vernier calipers. The speed of light is then found from the slope of a  $\Delta L$  versus  $1/\Delta f$  plot. The unknown details of  $n_{\text{HeNe}}$ ,  $L_{\text{HeNe}}$ , and similar terms for the glass window are gathered in the  $y$ -intercept. This algebraic trick works only when the laser is in the  $\text{TEM}_{00}$  mode, and does not work if the laser were in transverse  $\text{TEM}_{Nij}$  modes (where  $i$  and  $j$  are nonzero), as represented in Eq. (3). More elegantly, we are taking the derivative of Eq. (2) in the region of air where we are free to move the output coupler as shown:

$$\frac{dL}{d\left(\frac{1}{\Delta f}\right)} = \frac{c}{2n_{\text{air}}}. \quad (5)$$

### B. Frequency Measurement

For the range of laser cavity lengths in the set-up ( $\approx 0.54$  m to  $0.38$  m), the beat frequency varies from  $\approx 280$  MHz to  $390$  MHz, a change of  $110$  MHz over  $16$  cm. The signal from the photodetector was analyzed with an RF spectrum analyzer with a maximum span of  $3$  GHz and a minimum resolution bandwidth of  $10$  Hz.[5, 8] A frequency counter could in principle be used, but would not provide insight into additional beat frequencies from transverse mode contributions. In addition to analyzing

the laser output with the photodetector and spectrum analyzer, we split off a portion of the laser output to a scanning Fabry-Perot interferometer to observe its longitudinal mode structure.[20] The Fabry-Perot spectrum shows the number of modes and their amplitudes (and therefore the amplitude of the gain curve).

The amplitude of the modes provides information on frequency pulling and pushing, which cause small but statistically significant shifts in the beat frequency. *Frequency pulling* refers to a change in the spacing of longitudinal modes under a gain curve resulting from the different indices of refraction experienced by each mode. Across the range of frequencies that lie within the laser gain curve, the index of refraction varies steeply near the resonance transition, being lower or higher for frequencies below or above the resonance transition. From Eq. (2) we see that the allowed frequencies below the gain peak occur at higher frequencies than would be expected and vice versa. The result is a ‘‘pulling’’ of the longitudinal modes toward the center of the gain curve, effectively decreasing the difference frequency between the two. The amount by which the modes are pulled together and the beat frequency is lowered is a function of the relative intensity of the two heterodyning modes. For a given gain curve amplitude we find that the beat frequency varies over  $\approx 30$  to  $40$  kHz for the full range of mode relative intensities, in agreement with other studies.[21]

*Frequency pushing* refers to the increase of the difference frequency between longitudinal modes as the field intensity in the laser cavity increases.[22, 23] As the gain in the cavity is increased, the beat frequency also increases. We observe this increase in our set-up; when two adjacent longitudinal modes are observed with identical intensities, for a  $\approx 10\%$  change in total amplitude of the gain curve, there is a  $\approx 9$  kHz change in beat frequency. Figure 3 shows this effect over a wide range of amplitudes, showing a linear relation between the change in the intensity of the modes and the frequency pushing effect. When taking data to measure the speed of light, we are able to hold our amplitude fluctuation to a variation of  $\pm 10\%$ .

To minimize inconsistencies due to frequency pulling effects, we use the Fabry-Perot to ensure that each measurement (that is, the beat frequency at each cavity length) is taken for two longitudinal modes at the same relative intensities (see Fig. 4). The refractive index within the laser tube is then the same for both modes and very similar for all beat frequency measurements, reducing the pulling effect. More complex methods of ensuring that the two longitudinal modes are symmetric about the frequency of the emission line have been implemented in other studies.[24] These involve using a non-Brewster window laser and subtracting the outputs of the orthogonal modes detected with two photodetectors and a polarizing beam splitter. This difference is used to control the electronic feedback to make slight adjustments to the length of the cavity. We have not attempted such elaborate feedback schemes. Instead, students make

the necessary adjustments by applying gentle pressure to the optical table, which affects the cavity length on the micron scale.

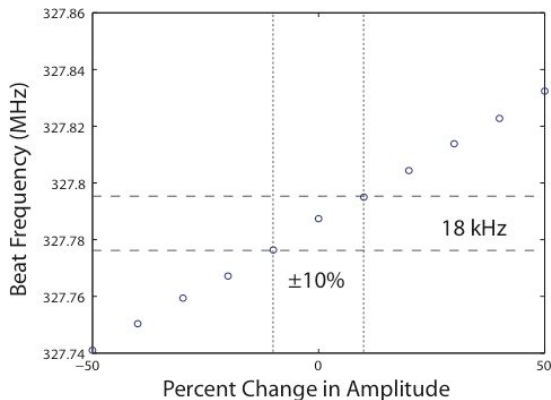


FIG. 3: A sample plot of beat frequency as a function of gain curve amplitude as read from the Fabry-Perot transmission showing the effects of frequency pushing. The uncertainty in the gain curve amplitude of  $\pm 10\%$  corresponds to a 18 kHz frequency variation equivalent to a  $\pm 9$  kHz uncertainty in the beat frequency. The 0% mark in this figure refers to the desired amplitude at which the frequency measurement is to be taken.

To counteract inconsistencies due to frequency pushing effects, we use the Fabry-Perot to ensure that each measurement is taken with the longitudinal modes at the same total amplitude and thus at the same laser intensity (see Fig. 5). The laser power is controlled by changing the cavity loss by adjusting the intra-cavity iris.

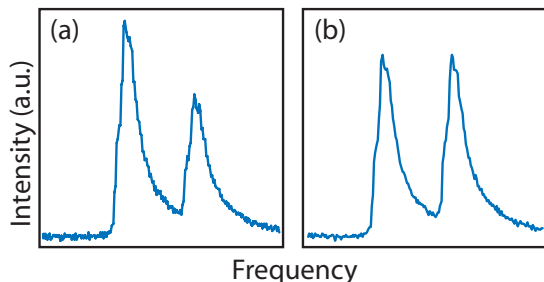


FIG. 4: Screen shots from the oscilloscope showing transmission of the scanning Fabry-Perot interferometer. The laser output power is the same in both cases. (a) An instance where the two mode intensities are asymmetrical around the center of the gain curve, whereas (b) shows the two modes when they have equal intensities. Due to frequency pulling, the two instances will produce beat frequency values differing by a few kHz.

### III. DATA ANALYSIS AND RESULTS

Figure 6 represents experimental data for 28 cavity lengths. The uncertainty in our  $\Delta L$  measurement is

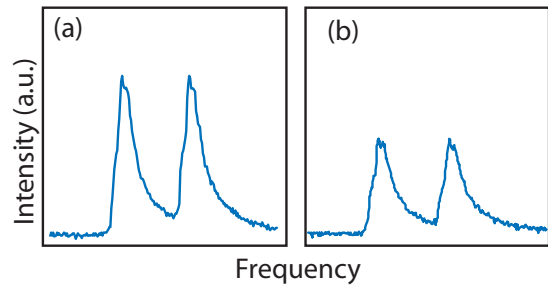


FIG. 5: Screen shots from the oscilloscope showing transmission of the scanning Fabry-Perot interferometer. Both show the existence of two longitudinal modes at the same relative intensity and thus each exhibit the same frequency pulling induced effects. (a) Two modes when the laser is operating at a higher gain setting than is present in (b). Due to frequency pushing, the beat frequency produced by the modes in (a) is higher than the beat frequency produced by the modes in (b).

$\pm 1 \times 10^{-5}$  m, dictated by the measurement limit of the digital vernier calipers. The uncertainty in our beat frequencies is dominated by frequency variability due to frequency pulling and pushing and has been minimized with the use of the Fabry-Perot interferometer. Due to frequency pulling and pushing, a change in the relative or total intensities of the heterodyning longitudinal modes corresponds to a change in the beat frequency. Thus the uncertainty in the beat frequency is found by estimating the precision to which we can achieve both the desired mode relative intensity and desired gain curve amplitude. Using the Fabry-Perot interferometer, we find that we can steadily hold the two longitudinal modes at equal relative intensities, resulting in a negligible uncertainty of  $\approx \pm 2$  kHz due to frequency pulling. Most of the uncertainty comes from frequency pushing, for it is not as simple to hold the total amplitude of the gain curve at a fixed value. To estimate this uncertainty, the precision to which the amplitudes of the modes can be held constant is converted into an uncertainty in frequency from the spread of beat frequencies observed simultaneously on the spectrum analyzer. We observe that by adjusting the position and aperture size of the iris in the resonator, we can manipulate the output to have two longitudinal modes with equal intensity and an overall gain amplitude that is constant to within  $\pm 10\%$ . Figure 3 shows the beat frequency as a function of the total mode amplitude for our system. A  $\pm 10\%$  variation in the total mode amplitude corresponds to an uncertainty in a single measurement of the beat frequency of  $\pm 9$  kHz.

The uncertainty in the frequency measurement,  $\sigma_{\Delta f}$ , and the uncertainty in the length measurement,  $\sigma_{\Delta L}$ , are fixed for each data point, but the uncertainty in the reciprocal beat frequency,  $\sigma_{1/\Delta f}$ , is a function of  $\Delta f$  (which varies for each data point). Hence the uncertainty in  $1/\Delta f$  is not fixed for each data point:  $\sigma_{1/\Delta f} = \sigma_{\Delta f}/(\Delta f)^2$ . Additionally the equivalent uncertainty in  $\Delta L$  due to the uncertainty in  $\Delta f$  is of the same order of

magnitude as  $\sigma_{\Delta L}$ . That is,

$$\frac{d(\Delta L)}{d\left(\frac{1}{\Delta f}\right)} \sigma_{1/\Delta f} \approx \sigma_{\Delta L}. \quad (6)$$

For this reason, a weighted least squares regression incorporating uncertainty in both variables is performed for the  $\Delta L$  versus  $1/\Delta f$  data.[25]

The final result for the speed of light in air based on the data plotted in Fig. 6 is

$$c = (2.9972 \pm 0.0002) \times 10^8 \text{ m/s}. \quad (7)$$

The uncertainty of  $\pm 0.0002$  is small enough to discriminate between the speed of light in air ( $2.9971 \times 10^8$  m/s for  $n_{\text{air}} = 1.00027$ ) and the speed of light in a vacuum ( $2.9979 \times 10^8$  m/s).

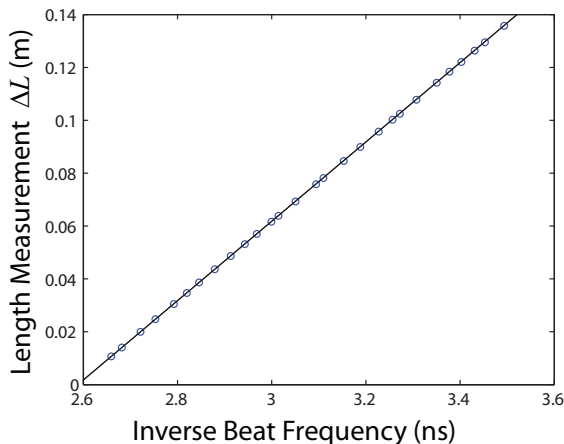


FIG. 6: The plot of 28 data points are fit using a weighted least squares regression. Errors are too small to display on this scale. We find a slope of  $c/2n_{\text{air}} = (1.4986 \pm 0.0001) \times 10^8$  m/s.

The measured speed of light yields an index of refraction for air in our lab of  $n_{\text{air}} = 1.00024 \pm 0.00006$ . We compare this value to the index of refraction of air as a function of temperature, wavelength, pressure, and humidity. At conditions of 20°C, 632.8 nm, 1 atm, and 40%

relative humidity, the accepted index of refraction of air is 1.00027.[26] No realistic changes in relative humidity, room temperature, or atmospheric pressure significantly affect the result. Therefore, the method described here does not have the necessary precision to demonstrate the effects of atmospheric fluctuations on the index of refraction.

#### IV. CONCLUSION

This experiment exposes students to a variety of experimental and mathematical techniques, demonstrates the importance of uncertainty in measurement, provides a meaningful context for using weighted regression, and familiarizes the student with three ubiquitous instruments: the laser, the Fabry-Perot interferometer, and the RF spectrum analyzer. In addition the experiment yields satisfying results, allowing measurement of the speed of light to a precision which differentiates between the speed of light in air and the speed of light in a vacuum. The precision to which the measurement is taken is limited by both the precision of our length measurement and our ability to minimize uncertainties due to the frequency pushing and pulling. One could improve length measurements with a precision linear stage and one could lock the HeNe laser so that the longitudinal modes are held to the same amplitude, but both of these improvements would be beyond the necessary scope of an intermediate physics laboratory course.

#### Acknowledgments

The authors would like to thank all of the Juniata College students who have performed this measurement in the Advanced Physics Lab over the past five years. The students that have been particularly instrumental in improving the experimental technique or data analysis have been included as authors. We also thank the reviewers for their insightful comments. This work has been supported by the von Liebig Foundation and NSF PHY-0653518.

- 
- [1] M. Csele, *Fundamentals of Light Sources and Lasers* (John Wiley & Sons, New York, New York, 2004).
  - [2] P. W. Milonni, and J. H. Eberly, *Lasers* (John Wiley & Sons, New York, New York, 1988) pp. 9–14, 505.
  - [3] F. L. Pedrotti, L. S. Pedrotti, and L. M. Pedrotti, *Introduction to Optics* (Pearson Education, Upper Saddle River, NJ, 2007), 3rd ed., pp. 153, 264–268.
  - [4] K. Razdan, D. A. Van Baak, “Demonstrating optical beat note through heterodyne experiments,” *Am. J. Phys.* **70**, 1061–1067 (2002).
  - [5] New Focus Visible Nanosecond Photodetector 1621 or

- Thorlabs Si Biased Detector DET10A.
- [6] R. A. Phillips and R. D. Gehr, “Laser mode structure experiments for undergraduate laboratories,” *Am. J. Phys.* **38**, 429–433 (1970).
- [7] R. S. Conroy, A. Carleton, A. Carruthers, B. D. Sinclair, C. F. Rae, and K. Dholakia, “A visible extended cavity diode laser for the undergraduate laboratory,” *Am. J. Phys.* **68**, 925–931 (2000).
- [8] All data presented here were acquired with an Agilent CSA model N1996A 3GHz Spectrum Analyzer. Less expensive alternatives have also been used, such as the

- Global Specialties 1GHz Spectrum Analyzer GSA1000.
- [9] R. G. Brickner, L. A. Kappers, and F. P. Lipschultz, "Determination of the speed of light by measurements of the beat frequency of internal laser modes," *Am. J. Phys.* **47**, 1086–1087 (1979).
- [10] See references in H. E. Bates, "Resource Letter RMSL-1: Recent measurements of the speed of light and the redefinition of the meter," *Am. J. Phys.* **56**(8), 682–687 (1988).
- [11] E. Gülmez, "Measuring the speed of light with a fiber optic kit: An undergraduate experiment," *Am. J. Phys.* **65**(7), 614–618 (1997).
- [12] L. Foucault, "Détermination expérimentale de la vitesse de propagation de la lumière," *Compt. Rend.* **55**, 501–503, 792–796 (1862).
- [13] R. Barr and T. R. Armstrong, "An inexpensive apparatus for the measurement of the group velocity of light in transparent media using a modified Helium-Neon Laser," *Am. J. Phys.* **58**, 1059–1064 (1990).
- [14] C. L. Tang and H. Statz, "Nonlinear effects in the resonant absorption of several oscillating fields by a gas," *Phys. Rev.* **128**(3), 1013–1021 (1962).
- [15] J. R. Brandenberger, *Lasers and Modern Optics in Undergraduate Physics – A Report to Foundations, Corporations, and Undergraduate Colleges* (Lawrence University, Appleton, Wisconsin, 1989), pp. 15–28.
- [16] W. F. Polik, "A hands-on helium-neon laser for teaching the principles of laser operation," in *Developing a Dynamic Curriculum Physical Chemistry*, edited by R. W. Schwenz and R. J. Moore (American Chemical Society, Washington, DC, 1993), pp. 84–108.
- [17] M. Jackson, D. Bauen, and J. E. Hasbun, "Investigation of laser fundamentals using a helium-neon laser," *Eur. J. Phys.* **22**, 211–218 (2001).
- [18] Kits with HeNe plasma tubes, with one or no internal mirror and windows (either straight or at the Brewster angle) as well as an output coupler and mounts, can be purchased from Melles Griot.
- [19] J. P. Goldsborough, "Beat frequencies between modes of a concave-mirror optical resonator," *Appl. Opt.* **3**(2), 267–275 (1964).
- [20] Scanning Fabry Perot, Thorlabs SA200-5B-SP. Free Spectral Range: 1.5 GHz; Finesse: 250
- [21] A. M. Lindberg, "Mode frequency pulling in He-Ne Lasers," *Am. J. Phys.* **67**, 350–353 (1999).
- [22] A. E. Siegman, *Lasers*, (University Science Books, Sausalito, CA, 1986), pp. 1192–1194.
- [23] K. Shimoda, *Introduction to Laser Physics* (Springer-Verlag, New York, NY, 1986), 2nd ed., p. 204.
- [24] R. Balhorn, H. Kunzmann, and F. Lebowsky, "Frequency stabilization of internal-mirror helium-neon lasers," *Appl. Opt.* **11**(4), 742–744 (1972).
- [25] P. R. Bevington, and D. K. Robinson, *Data Reduction and Error Analysis for the Physical Sciences* (McGraw Hill, New York, NY, 2003), 3rd ed., pp. 101–111.
- [26] J. A. Stone and J. H. Zimmerman, NIST Metrology Engineering Toolbox, Index of Refraction of Air Vacuum Wavelength and Ambient Conditions Based on Modified Edlén Equation, <[emtoolbox.nist.gov/Wavelength/Edlen.asp](http://emtoolbox.nist.gov/Wavelength/Edlen.asp)>.